



ELSEVIER

December 1999

Materials Letters 41 (1999) 229–233

**MATERIALS  
LETTERS**

www.elsevier.com/locate/matlet

# Raman scattering of tetrahedrally-bonded amorphous carbon deposited at oblique angles

Minseo Park<sup>\*</sup>, S.M. Camphausen<sup>1</sup>, A.F. Myers<sup>2</sup>, P.T. Barletta, V. Sakhrani, L. Bergman, R.J. Nemanich, Jerome J. Cuomo

*Department of Materials Science and Engineering and Department of Physics, North Carolina State University, Raleigh, NC 27695, USA*

Received 30 March 1999; received in revised form 13 May 1999; accepted 13 May 1999

## Abstract

Amorphous carbon ( $t_x a-C_{1-x}$ ) films were prepared by filtered cathodic arc deposition (FCAD). The films were deposited on p-type Si (111). The angle of beam incidence was varied from  $0^\circ$  to  $75^\circ$  with respect to the substrate normal. Micro-Raman spectroscopy, electron energy loss spectroscopy (EELS), and transmission electron microscopy (TEM) were carried out for sample analysis. It was found that the position of the G peak shifts to a higher wave number region as the angle of incidence increases. This means that the  $sp^2/sp^3$  ratio increases with increasing angle. This conclusion is supported by EELS. The film deposited at an angle of  $75^\circ$  exhibits a columnar structure with alternating high and low carbon density regions. © 1999 Elsevier Science B.V. All rights reserved.

PACS: 78.66.Jg

Keywords: Amorphous carbon; Filtered arc depositors; Raman scattering; Electron energy loss spectroscopy

## 1. Introduction

Much interest has been shown in the deposition of tetrahedrally-bonded amorphous carbon due to its high hardness, chemical inertness to both acids and bases, wear resistance, and variability in optical band

gap depending on growth conditions [1–6]. This material exhibits many of the desirable properties of crystalline diamond, and yet it can be produced with ease at room temperature. Therefore, it can be useful for various electronic and tribological applications. Hydrogen-free tetrahedrally-bonded amorphous carbon can be produced by pulsed laser deposition [1,2], ion beam sputtering [3,4], and cathodic arc deposition [5,6].

Energetic carbon deposition by pulsed laser vaporization, cathodic arc, and ion beam sputtering at oblique angles has been investigated [7]. However, no Raman spectra from these samples were reported. Raman spectroscopy is a non-destructive evaluation

<sup>\*</sup> Corresponding author. E-mail: mpark2@eos.ncsu.edu

<sup>1</sup> Present address: Warner Lambert, 10 Leighton Road, Milford, CT 06460, USA.

<sup>2</sup> Present address: AMD, Sunnyvale, CA 94088, USA.

technique for structural analysis of various forms of amorphous carbon. In the present study, we have deposited amorphous carbon at oblique angles, and presented a systematic change in first-order Raman spectra of  $t_x a-C_{1-x}$  films as a function of incidence angle.

## 2. Experimental procedure

The amorphous carbon films were prepared by filtered cathodic arc deposition (FCAD). The films were deposited on p-type Si (111). Fig. 1 shows the diagram of the incident carbon ions on the substrate. The angle of beam incidence was varied from  $0^\circ$  to  $75^\circ$  with respect to the substrate normal. Detailed sample preparation procedures were published elsewhere [8]. The films were analyzed by micro-Raman spectroscopy, electron energy loss spectroscopy (EELS), and transmission electron microscopy (TEM). Micro-Raman spectroscopy was performed using backscattering geometry with the 514.5 nm line of an Ar ion laser. An ISA U-1000 scanning double monochromator was used to detect the first-order Stokes spectra. The size of the laser beam was  $\sim 5 \mu\text{m}$  in diameter. The EELS and TEM analyses were carried out using a Philips CM300 FEG TEM equipped with a Gatan model 666 parallel-acquisition EELS spectrometer.

## 3. Results and discussions

Fig. 2a, b, c, d and e show first-order Raman scattering of amorphous carbon ( $t_x a-C_{1-x}$ ) deposited at angles of  $0^\circ$ ,  $30^\circ$ ,  $45^\circ$ ,  $60^\circ$ , and  $75^\circ$ , respectively. The typical Raman spectrum of amorphous carbon consists of two broad bands; a D band (D for disordered) at approximately  $1350 \text{ cm}^{-1}$ , and a G band (G for graphite) at about  $1580 \text{ cm}^{-1}$ . The D band is associated with the disorder-induced  $A_{1g}$  mode at the K point in the Brillouin zone of the graphite [9]. When long-range translational symmetry is lost due to bond-angle disorder upon amorphization, the selection rule is destroyed. Thus, optical phonons with any  $k$  vector in the Brillouin zone can contribute to Raman scattering. The G band is related to the  $E_{2g}$  mode of the graphite [10]. The position and full width at half maximum (FWHM) of the peaks were obtained by fitting the peak with two Gaussian functions and a linear background.

In a typical Raman spectrum for amorphous carbon, the position of the G band shifts significantly if  $sp^2/sp^3$  ratio of the film varies [11,12]. The shift in frequency of the Raman spectrum can be produced by changes in the force constant. In these spectra, it was found that the position of G peak shifts to a higher wave number region and the FWHM of the G peak decreases as the angle of incidence increases, as is summarized in Fig. 3. The intensity of the D peak

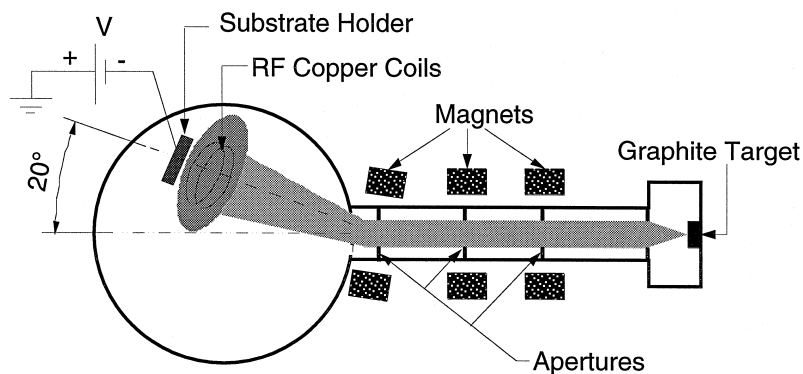


Fig. 1. Diagram of the incident carbon ions on the substrate.

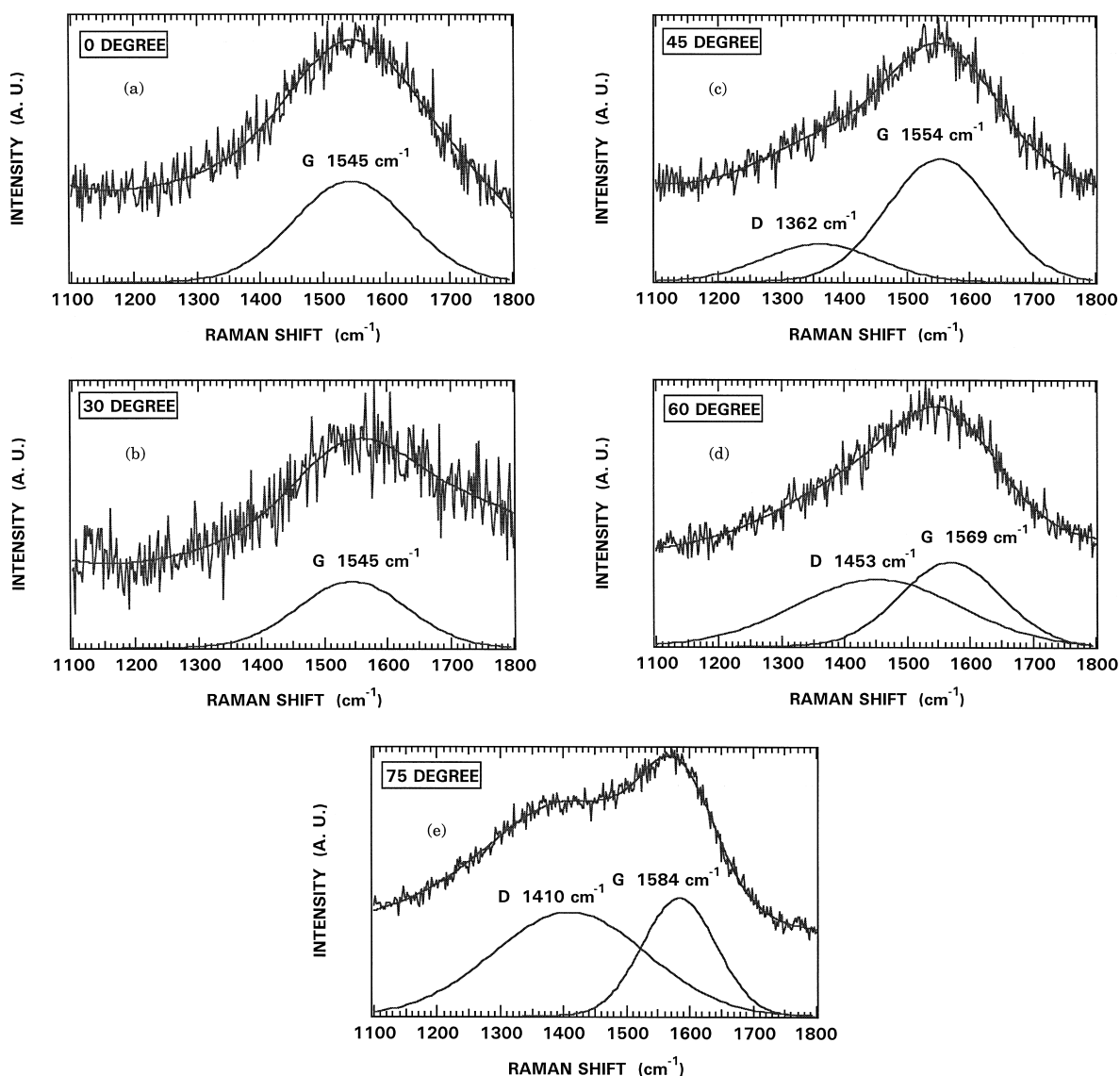


Fig. 2. First-order Raman scattering of amorphous carbon ( $t_x\text{a-C}_{1-x}$ ) deposited at an angle of (a)  $0^\circ$ , (b)  $30^\circ$ , (c)  $45^\circ$ , (d)  $60^\circ$  and (e)  $75^\circ$ .

starts to increase when the incidence angle is higher than  $30^\circ$ . The position and FWHM of G and D peaks and integrated intensity ratio  $I_D/I_G$  are summarized in Table 1.

The contributions from amorphous  $\text{sp}^3$  bonded carbon were not observed using laser with 514.5 nm line due to its low scattering cross-section [13]. Rather, UV excitation should be used to sufficiently excite the transition from  $\sigma$  to  $\sigma^*$  state in amor-

phous  $\text{sp}^3$  bonded carbon [14]. However, the excitation at 514.5 nm which is used in the present study is suitable for inducing resonant enhancement of the Raman cross-section of the amorphous  $\text{sp}^2$  species, since 514.5 nm corresponds to the transition between  $\pi$  and  $\pi^*$  states [15–17].

EELS was carried out with these samples since a smaller probe size ( $< 100 \text{ \AA}$ ) can be used in EELS than that in micro-Raman spectroscopy. The EELS

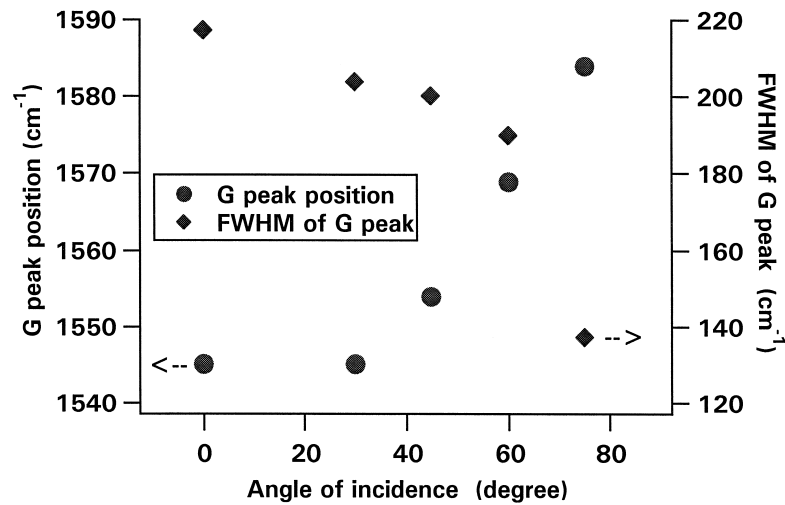


Fig. 3. Plot of the G peak position and FWHM of G peak with respect to the angle of incidence.

analysis can also provide quantitative information on the  $sp^3/sp^2$  ratio in the films. Bruley's "two-window" method was used for quantification [18]. The calculated  $sp^3$  carbon concentration in the films deposited at  $0^\circ$  and  $60^\circ$  are  $90(\pm 10)\%$  and  $30(\pm 10)\%$ , respectively. This means that the fraction of  $sp^2$  carbon increases as the angle of incidence increases.

Fig. 4 shows a cross-sectional TEM micrograph of  $t_x a-C_{1-x}$  films prepared at an angle of  $75^\circ$ . A selected area electron diffraction (SAED) pattern (which is not shown in this paper) confirmed that the film is amorphous in nature. It is well known that columnar microstructure can occur in amorphous Si and Ge [19]. A columnar structure with alternating high and low carbon density regions can be clearly seen from the TEM micrograph. It is believed that

each column is composed of mixture of  $sp^2$  and  $sp^3$  bonded carbon with different ratio. The formation of columnar structure can be explained by shadowing effect which follows the tangent rule [20];

$$\tan \alpha = 2 \tan \beta$$

where  $\alpha$  is the angle between source direction and substrate normal, and  $\beta$  is the angle between the columns and substrate normal. As the angle of incidence increases, the tendency to form a columnar structure increases. At a higher angle, the incoming atoms and ions will lose energy after experiencing multiple collision before landing. These atoms and ions may not have enough energy to produce highly  $sp^3$  bonded carbon. Therefore, it can be concluded that the formation of  $sp^2$  bonded carbon is promoted as the incidence angle increases. In this research, this

Table 1

The position and FWHM of G and D peaks, integrated intensity ratio  $I_D/I_G$ , and  $sp^3$  bonding fraction

Angle of incidence ( $^\circ$ )	$\nu_D$ ( $cm^{-1}$ )	$\nu_G$ ( $cm^{-1}$ )	$FWHM_D$ ( $cm^{-1}$ )	$FWHM_G$ ( $cm^{-1}$ )	$I_D/I_G$	$sp^3$ bonding fraction (%)
0		1545		217		$90(\pm 10)$
30		1545		204		
45	1362	1554	212	200	0.3	
60	1453	1569	309	190	1.3	$30(\pm 10)$
75	1410	1584	285	137	1.8	

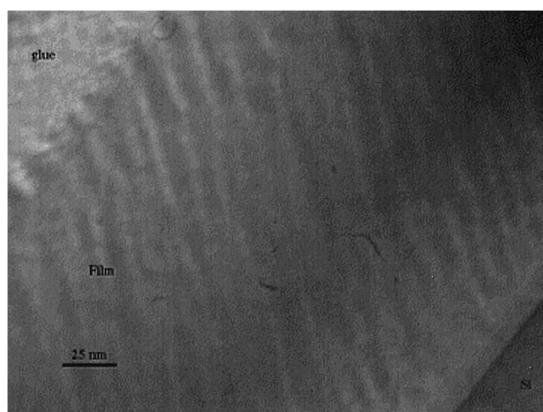


Fig. 4. A TEM micrograph of the cross-sectional view of  $t_x$ -a-C $_{1-x}$  deposited at angle of 75°.

phenomenon was well confirmed by Raman spectroscopy and EELS. The detailed mechanisms on the formation of the columnar structure was discussed elsewhere [21].

#### 4. Conclusions

The position of G peak shifts to a higher wave number region as the angle of incidence increases. This means that the  $sp^2/sp^3$  ratio increases with increasing angle. This conclusion is supported by EELS.

#### Acknowledgements

The authors would like to thank Dr. J.J. Hren for the numerous discussions. We also want to thank Dr. E.S. Etz at National Institute of Standards and Technology for invaluable comments on this manuscript.

#### References

- [1] S.S. Wagal, E.M. Juengerman, C.B. Collins, *Appl. Phys. Lett.* 53 (1988) 187.
- [2] D.L. Pappas, K.L. Saenger, J. Bruley, W. Krakow, J.J. Cuomo, T. Gu, R. Collins, *J. Appl. Phys.* 71 (1992) 5675.
- [3] J.J. Cuomo, J.P. Doyle, J. Bruley, J.C. Liu, *J. Vac. Sci. Technol., A* 9 (1991) 2210.
- [4] J.J. Cuomo, J.P. Doyle, J. Bruley, J.C. Liu, *Appl. Phys. Lett.* 58 (1991) 466.
- [5] R. Lossy, D.L. Pappas, R.A. Roy, J.J. Cuomo, V.M. Sura, *Appl. Phys. Lett.* 61 (1992) 171.
- [6] P.J. Martin, S.W. Filipczuk, R.P. Netterfield, J.S. Field, D.F. Whitnall, D.R. McKenzie, *J. Mater. Sci. Lett.* 7 (1988) 410.
- [7] J.J. Cuomo, D.L. Pappas, R. Lossy, J.P. Doyle, J. Bruley, G.W. Di Bello, W. Krakow, *J. Vac. Sci. Technol., A* 10 (1992) 3414.
- [8] S.M. Camphausen, A.F. Myers, S.P. Bozeman, D.A. Baldwin, J.J. Cuomo, *Mater. Res. Soc. Symp. Proc.* 498 (1998) 135.
- [9] F. Tuinstra, J.L. Koenig, *J. Chem. Phys.* 53 (1970) 1126.
- [10] R.J. Nemanich, S.A. Solin, *Phys. Rev. B* 20 (1979) 392.
- [11] A. Richter, H.-J. Scheibe, W. Pompe, K.-W. Brzezinka, I. Mühlhng, *J. Non-Cryst. Solids* 88 (1986) 131.
- [12] S. Prawer, K.W. Nugent, Y. Lifshitz, G.D. Lempert, E. Grossman, J. Kulik, I. Avigal, R. Kalish, *Diamond Relat. Mater.* 5 (1996) 433.
- [13] M. Geis, M.A. Tamor, in: G. Trigg (Ed.), *Encyclopedia of Applied Physics*, Vol. 15, VCH, 1993.
- [14] K.W.R. Gilkes, H.S. Sands, D.N. Batchelder, J. Robertson, W.I. Milne, *Appl. Phys. Lett.* 70 (1997) 1980.
- [15] M. Yoshikawa, G. Katagiri, H. Ishida, A. Ishitani, T. Akamatsu, *Appl. Phys. Lett.* 52 (1988) 1639.
- [16] J. Wagner, M. Ramseiner, C. Wild, P. Koidl, *Phys. Rev. B* 40 (1989) 1817.
- [17] M. Ramsteiner, J. Wagner, *Appl. Phys. Lett.* 51 (1987) 1355.
- [18] J. Bruley, D.B. Williams, J.J. Cuomo, D.P. Pappas, *J. Microsc.* 180 (1995) 22, Part 1.
- [19] R. Messier, A.P. Giri, R. Roy, *J. Vac. Sci. Technol., A* 2 (1984) 500.
- [20] J.M. Nieuwenhuizen, H.B. Haanstra, *Philips Tech. Rev.* 27 (1966) 87.
- [21] M.Q. Ding, A.F. Myers, W.B. Choi, R.D. Vispute, S.M. Camphausen, J. Narayan, J.J. Cuomo, J.J. Hren, *J. Vac. Sci. Technol. B* 15 (1997) 840.